

# **F61/62: Nuclear Magnetic Resonance**

**Yajie Liang and Leon Tschesche**

supervised by: **Alena Harlenderova**

on February 20<sup>th</sup>/ 21<sup>th</sup> 2019

handed in as short report on: June 3, 2019

## **Abstract**

blabla abstract

# Contents

<b>1</b>	<b>Introduction</b>	<b>2</b>
1.1	Basics of Nuclear Magnetic Resonance . . . . .	2
1.2	Relaxation time . . . . .	3
1.2.1	Spin-spin relaxation time $T_2$ . . . . .	3
1.2.2	Spin-lattice relaxation time $T_1$ . . . . .	4
1.3	Chemical shift . . . . .	4
1.4	Imaging with NMR . . . . .	5
<b>2</b>	<b>Layout of the experiment</b>	<b>6</b>
2.1	Relaxation Time and Chemical Shift . . . . .	6
2.2	Imaging with NMR . . . . .	7
<b>3</b>	<b>Measurements and evaluation</b>	<b>7</b>
3.1	Measurement of relaxation time . . . . .	7
3.2	Chemical shift . . . . .	8
3.3	Imaging with NMR . . . . .	8
3.3.1	1d imaging . . . . .	8
3.3.2	2d imaging . . . . .	8
<b>4</b>	<b>Discussion</b>	<b>8</b>

# List of Figures

1	Dephasing of transverse magnetization $\vec{M}_\perp$ . . . . .	3
2	Chemical Shift . . . . .	4
3	One of the N Loops needed for 2D Imaging . . . . .	5
4	The minispec p20, electronic unit on the left, magnetic unit on the right . . . .	6
5	Example of the used Labviews . . . . .	6
6	The NMR analyzer and LabView for 2D imaging . . . . .	7

# 1 Introduction

## 1.1 Basics of Nuclear Magnetic Resonance

Nuclear Magnetic Resonance, or short NMR, can only be observed for molecules with a non-zero magnetic dipole moment. For a given nuclei, whose spin  $\vec{J}$  is unequal to 0, one can calculate its magnetic dipole moment as

$$\vec{\mu} = \hbar\gamma\vec{J}. \quad (1)$$

Where  $\gamma$  is the gyromagnetic factor. In this experiment we will look at exclusively protons, which have  $\gamma_{proton} = 2.6752 \cdot 10^8 \text{sec}^{-1} \text{Tesla}^{-1}$ .

The magnetization of  $N$  nuclei can be obtained, by summing over all nuclei per unit volume

$$\vec{M} = \frac{1}{V} \sum_{i=1}^N \vec{\mu}_i \quad (2)$$

With the assumption of a weak field ( $\mu B \ll kT$ ), which is the case in our experiment, one can approximate  $\vec{M} \sim \frac{\vec{B}_0}{T}$  according to Curie's Law.

In general, the magnetization can have an arbitrary direction relative to the external field. In the following we will decompose it into the components  $\vec{M}_{\parallel}$  (anti-)parallel and  $\vec{M}_{\perp}$  perpendicular to the external field. The magnetic dipole interacts with the  $\vec{B}_0$  and as a result the general state of magnetization will dissipate its excitation energy and reach the ground state, i.e.  $\vec{M}_{\parallel}$ , asymptotically on a characteristic time scale. The dissipated energy can be expressed by

$$\Delta E = -\vec{\mu} \cdot \vec{B}_0 \quad (3)$$

This interaction results in a torque and since  $\vec{B}_0$  is parallel to  $\vec{M}_{\parallel}$ , the torque only acts on  $\vec{M}_{\perp}$ .

$$\vec{\tau} = \vec{M} \times \vec{B}_0 \quad (4)$$

Without a relaxation processes, the rate of change is given by

$$\frac{d\vec{M}_{\perp}}{dt} = -\gamma \vec{M}_{\perp} \times \vec{B}_0. \quad (5)$$

This differential equation can be solved by an Ansatz  $\vec{M} = M_{\parallel}(\cos(\omega_L t), \sin(\omega_L t), 0)$  with  $\omega_L$  being the Larmor frequency

$$\omega_L = \gamma B_0 \quad (6)$$

Let's consider the ground state magnetization  $\vec{M}$ , which is parallel to  $\vec{B}_0$  and the z-axis. If we apply a sinusoidal voltage with frequency  $\omega_{HF}$  to a coil which is coiled along the x-axis, it will result in a solenoidal magnetic field  $\vec{B}_1$  which is perpendicular to  $\vec{B}_0$ . This will lead to  $\vec{M}$  precessing around  $\vec{B}_1$ . During a time interval  $\Delta t$  the angle  $\alpha$  of the precession is then

$$\alpha = \gamma B_1 \Delta t. \quad (7)$$

If the time interval is chosen such that  $\alpha = 90^\circ$ , then  $\vec{M}$  is rotated into a perpendicular component  $\vec{M}_{\perp}$  along the y-axis. Such a pulse is called a  $90^\circ$  pulse. Similarly we define  $180^\circ$  pulse which results in magnetization antiparallel to the static field  $\vec{B}_0$ .

## 1.2 Relaxation time

Now we want to consider the relaxation process, which can be described with the Bloch equations. Here we introduce the rotating frame of the transverse magnetization, where the transverse magnetization is constant, if no relaxation processes takes place. The Bloch equations assume that the time evolution is dominated by a restoring force which is proportional to the deflection from equilibrium

$$\frac{dM_{\perp}(t)}{dt} = -\frac{M_{\perp}(t)}{T_2} \quad (8)$$

$$\frac{dM_{\parallel}(t)}{dt} = -\frac{M_{\parallel}(t) - M_0}{T_1} \quad (9)$$

where  $T_2$  is the spin-spin relaxation time,  $T_1$  the spin-lattice relaxation time and  $M_0$  the ground state magnetization.

In the laboratory system we can now write the equation (5) with (8) and (9) as

$$\frac{dM_{\perp}(t)}{dt} = -\frac{M_{\perp}(t)}{T_2} + \gamma(\vec{B} \times \vec{M})_{\perp} \quad (10)$$

$$\frac{dM_{\parallel}(t)}{dt} = -\frac{M_{\parallel}(t) - M_0}{T_1} + (\vec{B} \times \vec{M})_{\parallel} \quad (11)$$

### 1.2.1 Spin-spin relaxation time $T_2$

Spin-spin relaxation is caused by the interaction between different magnetic dipoles and it contributes to the transverse magnetization. This relaxation process is described by (10), which is solved by

$$M_{\perp}(t) = M_{\perp}^0 e^{-\frac{t}{T_2}}. \quad (12)$$

There are 2 methods for measuring  $T_2$ , which use similar techniques. First let's look at the spin-echo method. We apply a  $90^\circ$  pulse at  $t = 0$  to generate a transverse magnetization  $\vec{M}_{\perp}$ . We then wait for a time  $\tau$ , after which we apply a  $180^\circ$  pulse and wait till  $t = 2\tau$ . At that time the magnetization should be transverse polarized again and we can measure the loss of amplitude. The described process is visualized in the following figure.

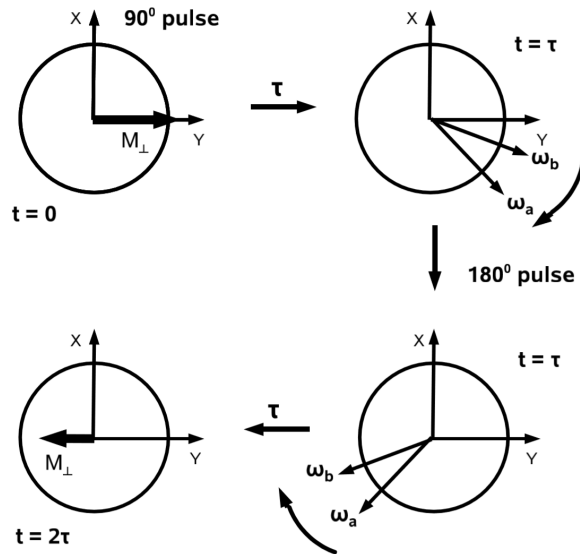


Figure 1: Dephasing of transverse magnetization  $\vec{M}_{\perp}$

$\omega_a$  and  $\omega_b$  are denoting 2 protons which experience different  $\omega_L$ 's, which is caused by the inhomogeneities of the external  $\vec{B}_0$ .

To measure the loss of amplitude we analyse the Fourier spectrum at the time  $t = 2\tau$  and integrate over the peak at the  $\omega_L$ . If we repeat the process for different  $\tau$  we will get a curve. This curve should follow (12), since the calculated amplitude is proportional to  $\vec{M}_\perp$ , and with the help of a fit we can extract the  $T_{2,SE}$ .

For the second method, the Carr-Purcell method, we also apply a  $90^\circ$  pulse at first and apply a  $180^\circ$  pulse at  $t = \tau$ . At  $t = 2\tau$  the system should be in phase, but will dephase shortly after, same as in method one. We then apply another  $180^\circ$  at  $t = 3\tau$  which will lead to a fully in phase system at  $t = 4\tau$  again. This process can be continued for  $180^\circ$  at odd multiples of  $\tau$  to get the system in phase at even  $\tau$ . This process is a lot more precise for big  $\tau$  in comparison to the spin-echo method, which gets inaccurate because of the molecular diffusion (the protons move away from their original position) and inhomogeneities in the field.

The measured amplitudes should still follow (12).

### 1.2.2 Spin-lattice relaxation time $T_1$

Spin-lattice relaxation is caused by the interaction between the magnetic dipoles and the external magnetic field  $\vec{B}_0$  and contributes to the parallel magnetization. This relaxation process is described by (11), which is solved by

$$M_{\parallel}(t) = M_0(1 - 2e^{-\frac{t}{T_1}}). \quad (13)$$

We measure  $T_1$  also with the spin-echo method. But this time we start at  $t = 0$  with a  $180^\circ$  pulse and follow up after  $t = \tau$  with a  $90^\circ$  pulse. We then measure the amplitude at  $t = 2\tau$  for different  $\tau$  and expect the resulting curve to follow (13).

## 1.3 Chemical shift

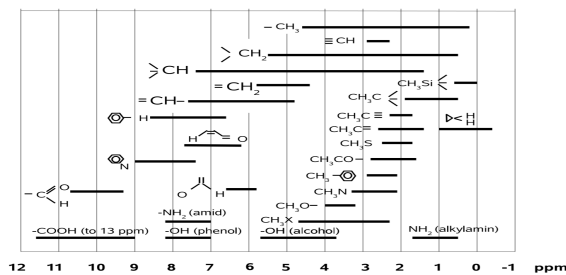


Figure 10: Chemical shifts  $\delta_i$  of compounds relative to TMS.

(a) Chemical Shift  $\delta_i$

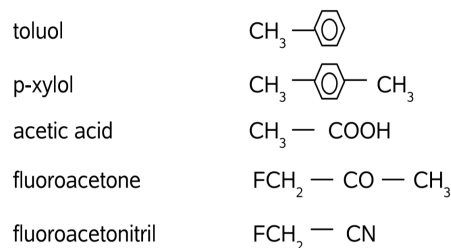


Figure 11: Five substances for identification.

(b) Substances to be sorted

Figure 2: Chemical Shift

If a proton is bound by a molecule, it will experience a magnetic field that is weaker than the external magnetic field  $\vec{B}_0$ , since the electrons are shielding parts of it. This leads to a new resonance frequency  $\omega_i$  for the proton bound by the molecule. This modified resonance frequency can be used to identify unknown substances. To do so, it is easiest to compare it to a reference substance which you can easily identify in a Fourier spectrum, since the whole frequency scale is dependent on  $\vec{B}_0$  which means it's a relative scale and one can't use absolute frequency values. We are using Tetra-Methyl-Silan or TMS since its peak will always be clearly visible and in our case always be the peak on the most left. With the help of  $\omega_{TMS}$  one can

define a chemical shift

$$\delta_i = \frac{\omega_{TMS} - \omega_i}{\omega_L} \quad (14)$$

for different molecule parts in reference to TMS as shown above in figure 2a. In this experiment we want to identify the substances in figure 2b from 5 different probes.

## 1.4 Imaging with NMR

Imaging with NMR is one of the most notable achievements of NMR. By adding a gradient to the external field  $\vec{B}_0$  we create a coordinate dependency of the  $B_0$  field, which implies a coordinate dependent  $\omega_L$ . There are two different approaches to determine the density of the NMR-active material of the probe in 1 dimension.

The first method is called frequency coding, where one has a fixed gradient over time and measures the NMR signal in set times  $t_n = n\Delta t$ . Then one can do a discrete Fourier transform of the  $N$  measurements and gets a finite amount of  $M_\perp(n\Delta z)$  for the different coordinates.

The second method is called phase coding, where one has a fixed time and determines the phase of the precession all at the same time  $t = t_0$ . From that you again get a discrete amount of data points with which you can do a discrete Fourier transform.

The main difference between these two methods is the time needed to record the data needed. The first method requires  $T_f = N \cdot \Delta t$  compared to the  $T_\Phi = t_0$  for the second method.

For 2 dimensions you have to use a combination of both since you need to determine 2 coordinates with just 1 signal. First a slice gets selected which is used to derive the positional information. Then it does phase coding for a set gradient while measuring the NMR signal over time with a set time distance  $t_m$ . After finishing the frequency coding it changes the gradient, selects a slice again and does a phase coding again followed by a frequency coding. This process is repeated for  $N$  different gradients, taking  $M\Delta t$  for each gradient. That leads to  $N \times M$  data points which then can be transformed with a 2 dimensional Fourier transform into the image matrix of the object. One of the  $N$  cycles is illustrated below 3.

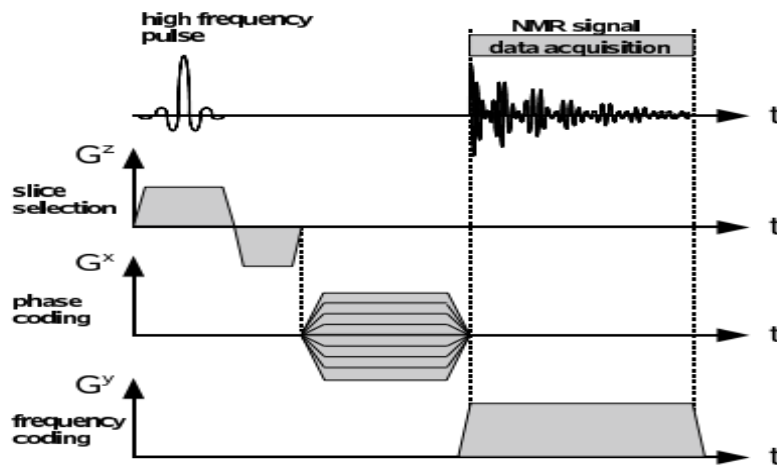


Figure 3: One of the  $N$  Loops needed for 2D Imaging

## 2 Layout of the experiment

### 2.1 Relaxation Time and Chemical Shift

For the first two parts of the this experiment we use a minispec p20 which produces both of the magnetic fields we need for the relaxation time and measuring the chemical shift.

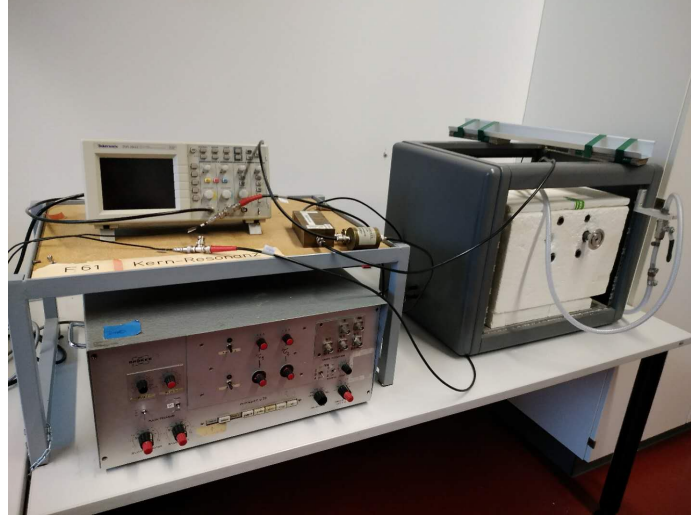


Figure 4: The minispec p20, electronic unit on the left, magnetic unit on the right

The constant  $\vec{B}_0$ , which is proportional to  $\omega_L$ , can be adjusted by turning the screw sticking out of the Styrofoam as seen in Figure 4 . The  $\omega_{HF}$  will be set by the electronic unit of the p20 seen on the left side of Figure 4. An oscilloscope is also provided to measure the characteristic time for a  $90^\circ$  pulse, which is needed to calibrate the electronic unit of the p20 for the relaxation time measurements. The tubes with the substances get inserted into the magnetic unit parallel to the screw used to change  $\omega_L$ . A high-pressure air nozzle can be used to rotate the tube to ensure a evenly distributed density of the substance in in the tube, we will use it for the chemical shift part since there only 1 measurement for each tube will be required.

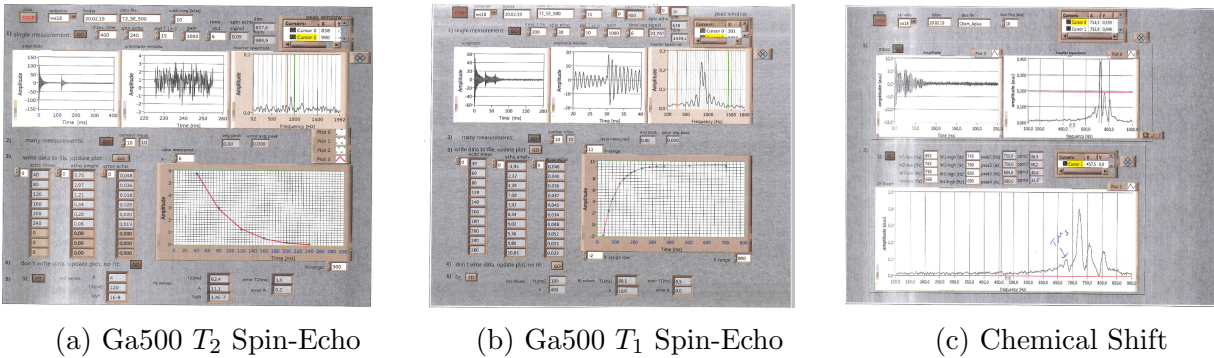


Figure 5: Example of the used Labviews

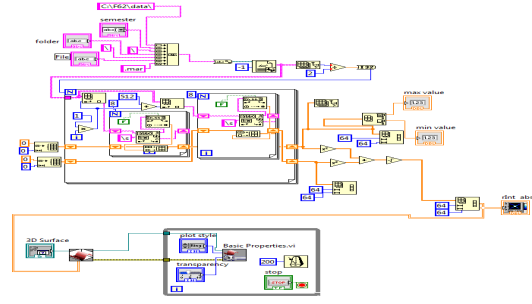
The data gets readout and analysed on a program written in Labview, the interface is shown in figure 5 via some example measurements.

## 2.2 Imaging with NMR

We use a Bruker NMR analyzer 7.5 to generate the magnetic fields needed for 1D and 2D imaging. The readout gets fed into a computer where it gets analysed and can be later on displayed with a LabView .vi, examples of both can be seen in figure 6.



(a) the Bruker NMR analyzer mq7.5



(b) LabView .vi to display 2d image

Figure 6: The NMR analyzer and LabView for 2D imaging

## 3 Measurements and evaluation

### 3.1 Measurement of relaxation time

We measure  $T_1$  and  $T_2$  once with the spin echo method and  $T_2$  again with the Carr-Purcell sequence for each Ga 500 and Ga 600.

Substance	$T_{1,SE}$	$T_{2,CP}$	$T_{2,SE}$
Ga 500	68.1	66.1	62.4
Ga 600	99.2	84.0	78.6

Table 1: Summary of relaxation time measurements in *ms*

We can see 3 relations from these measurements:  $T_1 > T_2$  and  $T_{2,CP} > T_{2,SE}$  for both substances as well as  $T_{600} > T_{500}$  for each different method.

The first can be explained by The second relation can be explained by looking at the effects of the Carr-Purcell method. This method minimizes the effects of the molecular diffusion and field inhomogeneities, which improves the precision of greater echo times.

The third relation can be attributed to the fact that the Ga 500 has higher concentration of hydrogen which leads to lower relaxation time .

From  $\omega_L = 19.8 \text{ MHz} \cdot 2\pi$  we can also calculate our external field  $\vec{B}_0$ . And with the characteristic time  $\Delta t = 1.29 \cdot 10^{-6}$  for a  $90^\circ$  pulse the solenoidal field  $\vec{B}_1$  as well.

$$B_0 = \frac{\omega_L}{\gamma} = 0.48T \quad (15)$$

$$B_1 = \frac{\alpha}{\Delta t \gamma} = 4.3mT \quad (16)$$

where  $\gamma$  was the gyromagnetic factor mentioned at the beginning for protons.



## 3.2 Chemical shift

We measure the peaks and determine which peak is the TMS. After that we calculate the shift with the given ppm of the .vi and appoint them to a substance from figure 2b with the help of the provided cheat-sheet seen in figure 2a.

	A+	B+	C+	D+	E+
$\Delta(2nd - TMS)$	2.2	2.1	2.0	3.9	2.6
$\Delta(3rd - TMS)$	3.9	6.9	11.6	6.3	7.5
$\Delta(4th - TMS)$	6.3				
Substance	fluoroacetone	p-xylol	acetic acid	fluoroacetonitril	toluol

Table 2: Summery of chemical shift in ppm

Even though the resonance frequency of Flour is a lot higher than the frequency we are using here, we can see the peaks caused by the Flour. They appear because the of the spin-spin interaction between Flour and the proton(hydrogen) in  $FCH_2$  which lead to 2 different states for the electrons. For both D+ and A+ we can see each of these peaks at 3.9 and 6.3 on both spectra.

From the width of these peaks we can additionally calculate the energy resolution of this measurement as well as the energy difference between the 2 different states  $FCH_2$  can be in depending on the spin-spin interaction of the electrons.

$$\Delta E_{res} = f_{FWHM} \cdot h = 19.9Hz \cdot 4.136eVs = 8 \cdot 10^{-14}eV \quad (17)$$

$$\Delta E_{dipole} = f_{\Delta F} \cdot h = 48Hz \cdot 4.136eVs = 2 \cdot 10^{-13}eV \quad (18)$$

## 3.3 Imaging with NMR

### 3.3.1 1d imaging

### 3.3.2 2d imaging

## 4 Discussion